A Real-Time Hardware Experiment Platform for Closed-Loop Electrophysiology

Weitong Liu, Siyuan Chang, *Graduate Student Member, IEEE*, Jiang Wang, *Member, IEEE*, and Chen Liu, *Member, IEEE*

***Abstract*— Targeted stimulation of nervous system has become an increasingly important research tool as well as therapeutic modality, and the stimulation signal acquisition based on the expected signal needs a closed-loop system. Due to the difficulty of biological experiments, the real-time simulation of neural activity is of great significance for the mechanism analysis and the performance improvement of neuromodulation techniques. This paper proposes a real-time hardware experimental platform for closed-loop electrophysiology. The platform integrates a neural computing module and a real-time control module on TMS320F28377D digital signal processors (DSP), and it reserves a programmable interface for users to call the required modules and set module parameters simultaneously. The platform has high compatibility and can be used for closed-loop electrophysiological experiments with different models, different control algorithms and different clamps. We implement the thalamocortical relay neural computing model and iteration improves proportional-integral algorithm on the platform for experimental verification in this paper. The neuron firing waveforms of the DSP platform and the MATLAB R2020b simulation waveforms are consistent. Under the same physiological time, the simulation speed of DSP platform is 3 times faster than that of the Intel Core i5-8400 CPU computer, and the neural firing rate of DSP platform is due to the real-time. This platform can be used as a tool to explore the working mechanism of the nervous system. It may promote the development of neuroscience, especially the field of closed-loop neuroscience.**

***Index Terms*— Hardware experimental platform, closed-loop electrophysiology, neural computing model, thalamocortical relay neural, iterative learning control.**

I. Introduction

THE human brain is a complex system of nearly 100 billion neurons and their synaptic connections. Exploring the working mechanism of the nervous system is not only an essential work of neuroscience but also a field with excellent exploration spaces at present [1]–[3]. For example, understanding the pathogenesis of nervous system diseases such as Parkinson's disease and the modulation mechanism of deep brain stimulation (DBS) on the nervous system will significantly improve the role of neural modulation technology in clinical treatment of nervous system diseases [4]–[8]. In addition, exploring the working mechanism of neurons will substantially promote the development of high-performance brain-like computing and a new generation of artificial intelligence [9]–[11].

Electrophysiological techniques based on *in vivo* or *in vitro* neural tissue provide a method to study the information processing mechanism of the nervous system [12]–[14]. Using the neural electrophysiological system and neural network *in vitro* culture technology, researchers can synchronously record the electrical activity signals of neural networks for a long time and apply various electrical stimuli to the neural network, which provides convenience for studying the input-output relationship of neural networks [15]–[19]. However, most such systems can only realize the fixed stimulus mode in open-loop form, explore the neural response under constant conditions, and lack the 'stimulus-response' feedback system, which partly limits the further research on the working mechanism of the nervous system [20], [21]. Moreover, the effect of open-loop stimulation is unstable since personalized control parameters need to be determined by the physician's experience in clinical treatment, and parameters need to be constantly adjusted as the condition progresses.

At the same time, closed-loop neuroscience has become a new idea to solve this problem [22], [23]. The combination of electrophysiological experiments and closed-loop mode can easily obtain the stimulus pattern corresponding to the desired neural activity [24]–[26]. The closed-loop electrophysiology system has the potential to provide a theoretical basis for choosing stimulus patterns for neural activity modulation. Proportional-integral (PI) control, fuzzy control, predictive control, and other algorithms have been successfully applied to obtain the optimal stimulus signal [26]–[30].

The software simulation is the primary tool in the past research of nervous system research, which still has many problems, such as calculation speed and practical usage. In contrast, hardware technology has the advantages of convenience, speed, accuracy, operation in real-time scale, high operation efficiency, and convenience for practical application.

Manuscript received November 11, 2021; revised December 22, 2021; accepted February 4, 2022. Date of publication February 9, 2022; date of current version February 18, 2022. This work was supported in part by the National Natural Science Foundation of China under Grant 62173241; in part by the Natural Science Foundation of Tianjin, China, under Grant 20JCQNJC01160; in part by the Foundation of Tianjin University under Grant 2020XRG-0018; and in part by the Opening Foundation of Key Laboratory of Opto-Technology and Intelligent Control (Lanzhou Jiaotong University), Ministry of Education, under Grant KFKT2020-01. *(Weitong Liu and Siyuan Chang contributed equally to this work.) (Corresponding author: Chen Liu.)*

The authors are with the School of Electrical and Information Engineering, Tianjin University, Tianjin 300072, China (e-mail: liuchen715@tju.edu.cn).

Digital Object Identifier 10.1109/TNSRE.2022.3150325

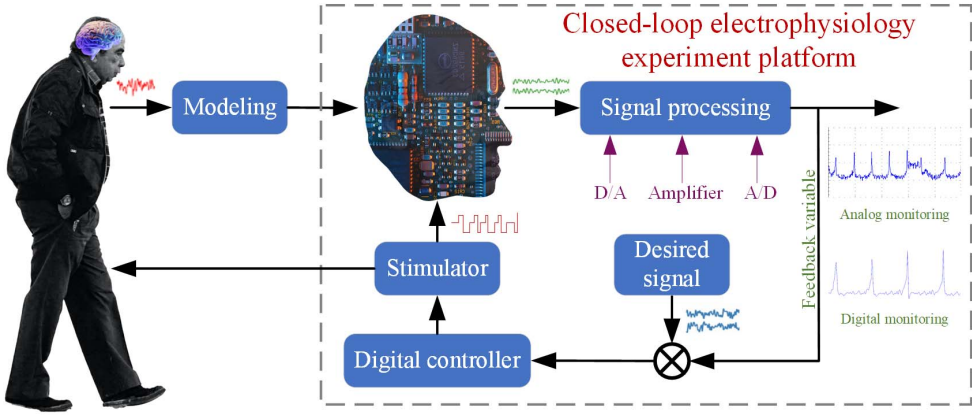

Fig. 1. **Schematic of closed-loop electrophysiology experiment platform.** The closed-loop electrophysiology experiment platform models the neural activities, and then uses the data that generated by the artificial neurons to verify and modulate the control strategies. Then the control strategies could be used into clinical treatment of nervous system disease and the exploration of the brain's mechanism.

Also, electronic neurons can be used in experimental research of neural networks, neural prostheses, detection and treatment of nerve diseases, and other fields [15], [31]–[33].

Therefore, this paper presents a closed-loop electrophysiological platform to provide a tool for researchers to find suitable stimulation and exploring mechanisms in the nervous system. The model simulation experiments are used to replace physiological experiments, and the platform is implemented on digital signal processor (DSP). The platform has high compatibility and can be used for closed-loop electrophysiological experiments with different models, different control algorithms and different clamps. Moreover, by using models that quantitatively reflect the characteristics of neurons, more explorations can be executed about the brain-machine interface, the pathological study of nervous system diseases, the treatment of nervous system diseases, and so on through the system.

The major contributions of this study are as follows:

(1) This paper presents a compatible closed-loop electrophysiological experiment platform for different experiments and implements it on DSP.

(2) A user interface that matches the platform is designed based on Visual Studio 2019, which can set the parameters of the algorithm and model.

(3) Hodgkin-Huxley-model-based thalamocortical (TC) relay neuron is implemented on the platform, and different experiments are designed to validate the system and the model.

Accordingly, this paper is organized as follows. In section II, brief introduction of the system and the hardware implementations of the TC relay neuron models are presented. Section III shows the detailed structure of the DSP-in-loop experimental system, and the control results of the system are illustrated. Finally, section IV gives the conclusions.

II. Methods

A. System Framework Description

Figure 1 shows the framework of closed-loop electrophysiology experiment platform. First, the activity of real brain is analyzed to extract the critical information to build artificial neurons, which can map the activity of real neurons.

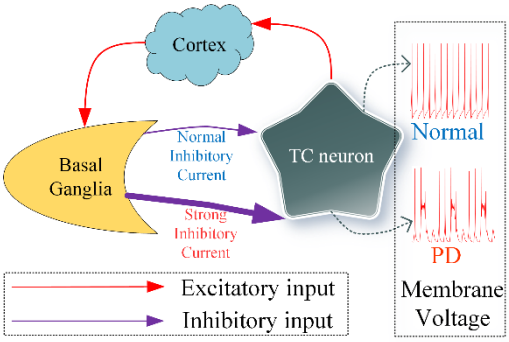

Fig. 2. **The cortico-basal ganglia-thalamocortical loop.** TC relay neuron connects the motor-cortexes. The inhibitory current of BG is stronger in parkinsonian state.

Many neuron models and neural network models have been developed and verified based on physiological experiments for research [34]–[36]. After the modeling, the digital signal generated by artificial neurons containing real neurons' activity will be fed into the closed-loop controller after the signal processing units. Subsequently, the stimulation signal will be sent to the modeled artificial neurons based on the feedback variable and the desired signals. Different experiments can be carried out on the platform to modulate the control strategy and the feedback variable, which helps to achieve better performance of controller. After that, the modulated controller can be used to stimulate real neurons in the future. In such a way, the activity patterns of the neurons and the control strategy to stimulate neurons can be explored, which will contribute to the study of neuroscience and the treatment of neural diseases.

B. TC Relay Neuron and Its Conductance-Based Biophysical Model

Figure 2 depicts the basal ganglia (BG)-thalamus circuit model, which is a significant structure spanning the telencephalon and diencephalon regions of the nervous system. The BG-thalamus circuit plays a vital role in behavioral selection, working memory, and other cognitive functions [37].

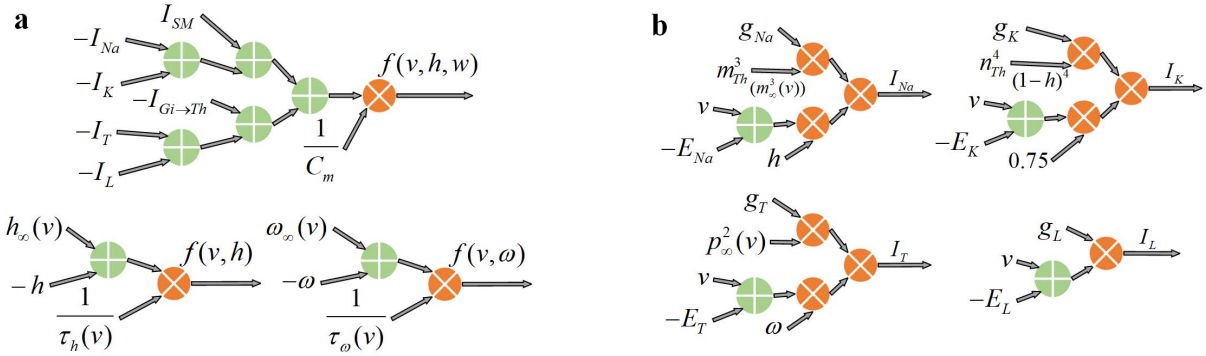

Fig. 3. **The detailed structure of the four-channel algorithm using fourth-order Runge-Kuta.** (a) The iterative equation of membrane potential and gated variables. (b) The detailed structure of the four types of ionic current in the TC neuron model.

TC neurons play a relay function between the cortex and thalamus in the BG circuit, responsible for both the functional relay of sensory information from the external surroundings to the cortex and the communication interface between cortical regions [38].

Proposed by Rubin and Terman, the TC neuron model is a single-compartment conductance-based model [39]. Many previous studies have verified and analyzed the model, which can better describe the activity characteristics of TC neurons [40], [41]. A set of Hodgkin-Huxley differential equations can interpret the dynamic characteristics of the TC relay neuron model, and the time evolution equation of membrane potential V is shown in the equation (1):

$$C_m \frac{dV}{dt} = -I_{Na} - I_K - I_T - I_L - I_{Gi\to TC} + I_{SM} \quad (1)$$

where C_m represents the membrane capacitance, and V represents the TC neuron membrane potential. I_{Na}, I_K, I_T, and I_L represent Na^+ current, K^+ current, low threshold T-type Ca^{2+} current, and leakage current, respectively. $I_{Gi\to TC}$ represents inhibitory synaptic current that from Globus Pallidus internus (GPi) of BG to thalamic nucleus. Finally, I_{SM} indicates the random or cyclical excitatory input information from the cortex to the thalamus.

The detailed descriptions and explanations about ion channels, gated variables, and excitatory input are in Appendix A.

C. The Implementation of the Closed-Loop Electrophysiological System

$$\begin{cases} V(n+1) - V(n) = \frac{V_1(n)}{6} + \frac{V_2(n)}{3} + \frac{V_3(n)}{3} + \frac{V_1(n)}{6} \\ V_1(n) = \Delta t * f(V(n), h(n), w_{Th}(n)) \\ V_2(n) = \Delta t * f(V(n) + \frac{1}{2}V_1(n), h(n) + \frac{1}{2}h_1(n), \ldots \\ \qquad w_{Th}(n) + \frac{1}{2}w_{Th1}(n)) \\ V_3(n) = \Delta t * f(V(n) + \frac{1}{2}V_2(n), h(n) + \frac{1}{2}h_2(n), \ldots \\ \qquad w_{Th}(n) + \frac{1}{2}w_{Th2}(n)) \\ V_4(n) = \Delta t * f(V(n) + V_3(n), h(n) + h_3(n), \ldots \\ \qquad w_{Th}(n) + w_{Th3}(n)) \end{cases} \quad (2)$$

The fourth-order Runge-Kutta is used to discretize the TC relay neuron model, which can approximate complex curves in a solving step size to obtain high computational accuracy through four-step piecewise approximation of differential equations. There are three blocks for the derivatives of the variable V and ω in their corresponding equations. The nonlinear ordinary differential equation of V is discretized into Equation (2). Where n represents the number of iterative steps. Δt represents the timestep in the fourth-order Runge-Kutta method which is also the discrete-time parameter.

In this work, Δt is the same both in the discrete process of MATLAB stimulation and DSP based experiments, which is 0.02 ms. The detailed structure of the four-channel algorithm using fourth-order Runge-Kutta is as Figure 3.

The discrete analysis of two gating variables h and ω is described in Appendix B.

III. Result

A model-based closed-loop electrophysiological system is developed, as depicted in Figure 4 (a). The system mainly includes host PC, DSP-based neuron model, closed-loop controller and corresponding signal transmission and detection circuit. Figure 4 (b) shows the signal flow graph of the closed-loop electrophysiological system.

The platform is implemented on TMS320F28377D DSP platform, which has two TMS320C28x 32-bit CPUs. Compared with field programmable gate array (FPGA), DSP has independent multiplier hardware, and multiplication instructions can be completed in a single cycle [42]. Therefore, DSP is faster calculating floating-point operation in neural network and control algorithm, and has better implementation ability of complex algorithm. The CPU of DSP can perform single-precision floating-point operation at 200 MHz, thus the chip takes 5 ns to perform an addition or multiplication operation. And the time that DSP takes to execute the code that calculates the difference equation of TC relay neuron once is about 450 clock cycles. Therefore, the calculated time of DSP is 0.23 μs, which is 3 times faster than that in MATLAB R2020b simulation. In MATLAB, the simulation step is set to 20 μs. Using this chip can meet the real-time requirements of the platform, and the calculation time of the platform is much shorter than the simulation step time, so that the implementation of multiple neurons can be extended on

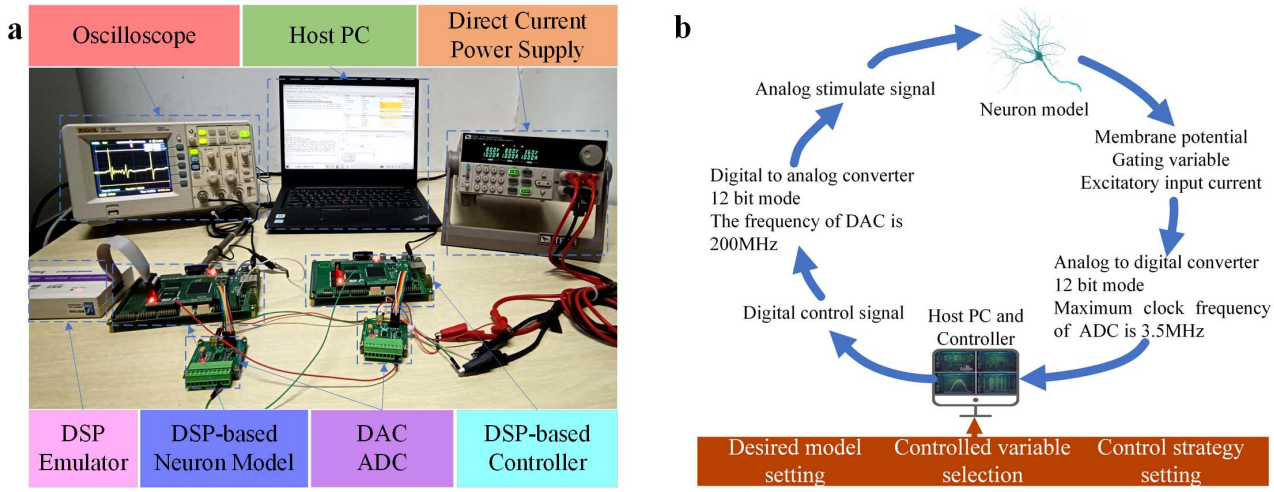

Fig. 4. **The overview of the closed-loop electrophysiology platform structure.** (a) The prototype of the closed-loop electrophysiological system, mainly includes host PC, DSP-based neuron model, closed-loop controller and corresponding signal transmission and detection circuit. (b) The signal flow graph of the closed-loop electrophysiological system.

this platform due to the excellent computing performance and scalability of DSP.

There are two DSPs in the platform. The first DSP realizes a high-precision virtual neuron that reflects the dynamic characteristics of the real neuron. The other DSP acts as the digital closed-loop controller, which receives neural activity information from the virtual neuron and then sends stimulation after algorithm calculation. The simulated neural activity signals of the artificial neuron is transmitted into a digital-to-analog converter (DAC) to generate analog rhythmic firing signals. Simultaneously, the artificial neuron receives the stimulation signals of the controller via analog-to-digital converter (ADC) to simulate the neural activity after receiving the stimulation. The 12-bit DAC converts 12-bit digital signals to analog signals, so the maximum decimal number corresponding to digital signals is 4095. And the clock frequency of the DAC is the same as the main frequency of the C28x core, which is 200 MHz. The 12-bit ADC converts analog signals to 12-bit digital signals and sends the digital signals to the result register. The maximum clock frequency of ADC is 3.5 MHz, and there is an independent sample-and-hold circuit to keep the signal constant for each ADC. In this work, the setting time of DAC is 1 μs, so that the throughput of DAC is 1 Msps. The ADC takes 15 ADC clock to sample and 10 ADC clock to convert signal, and the ADC clock frequency is 3.5 MHz, so that the sampling frequency is 140kHz. Both ADC and DAC can meet the needs of system.

The host PC sets and monitors the vital parameters of both models and the controller. The hardware platform and host PC are connected by serial communication interface (SCI), guaranteeing the high-speed bidirectional data transmission. The SCI is a full duplex serial communication interface and the host PC can transmit data with DSP in both directions through RS-232 interface. However, the SCI data buffer registers can only send up to 8-bit binaries at a time, whereas the data is 32-bit floating-point in high-precision DSP. Therefore, 32-bit floating-point data needs to be converted to string-type data, split up and sent one by one before data transfer. The user interface of the system has been implemented using Visual Studio 2019 as shown in Figure 5. The user interface consists of the following four functions: (1) showing the waveforms, (2) setting the parameters of the model, (3) changing the control strategy, (4) saving the data of the waveforms.

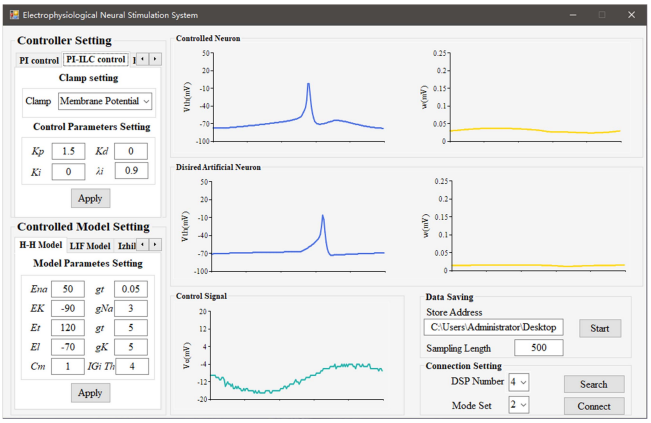

Fig. 5. **The user interface of the closed-loop electrophysiology system.** On the left panel of user interface, the control strategies and models can be switched, and the corresponding parameters can be set. The crucial signals can be monitored and saved on the right panel of user interface.

TABLE I
THE CORRESPONDING PARAMETERS OF TC RELAY NEURON MODEL

Parameter	Value	Parameter	Value
E_{Na}	50 mV	g_l	0.05 nS/μm^2
E_K	-90 mV	g_{Na}	3 nS/μm^2
E_t	120 mV	g_t	5 nS/μm^2
E_l	-70 mV	g_K	5 nS/μm^2
C_m	1 pF/μm^2	$I_{Gi\to TC}$	$0-5$ pA/μm^2

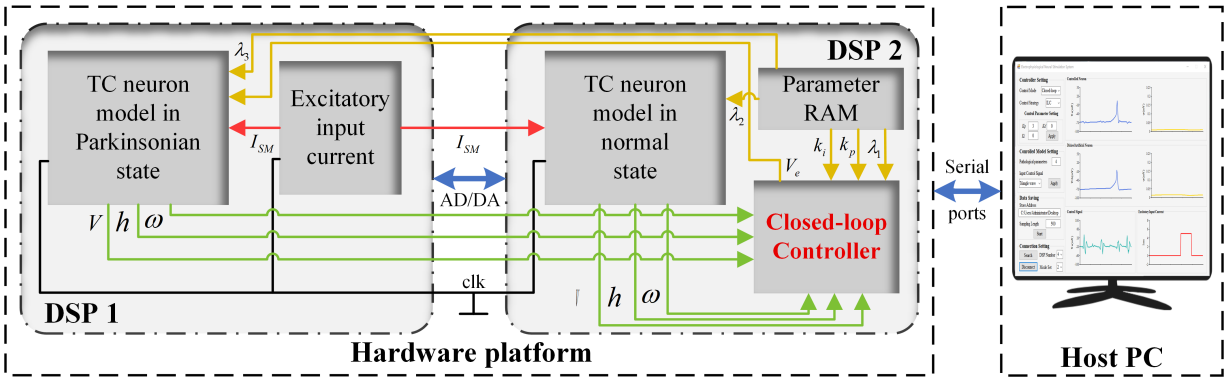

Fig. 6. **The implementation of TC relay neuron on the closed-loop electrophysiology system.** The hardware platform consists of the controlled model and the controller. The host PC sets the parameters and monitors the vital signals of models. V is the membrane potential, ω is the gating variable, V_e is the stimulation signal. TC relay neuron model in parkinsonian state is designed as the controlled neuron due to its abundant dynamics, and the normal TC relay neuron in DSP2 generates the desired signals.

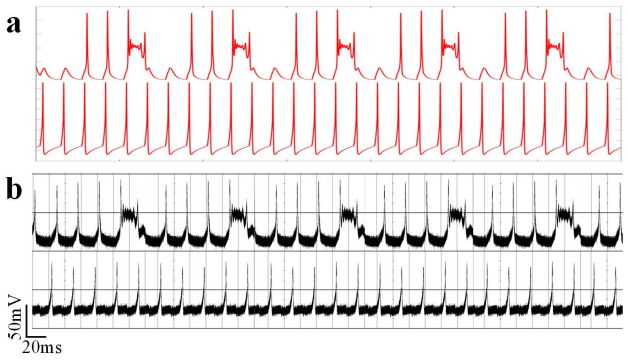

Fig. 7. **The membrane potential V of TC relay neuron both in parkinsonian state and normal state.** (a) MATLAB simulation diagram. (b) Analog oscilloscope picture generated by the hardware platform.

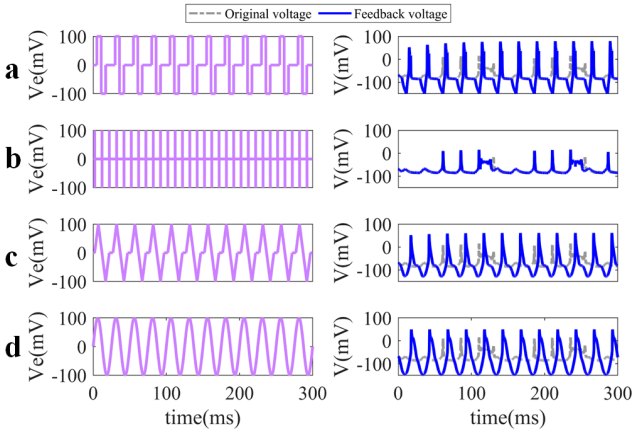

Fig. 8. **The open simulation of TC relay model.** V_e is the stimulation signal, V is the membrane potential. (a) The square stimulation waves. (b) The impulse stimulation waves. (c) The triangle stimulation waves. (d) The sine stimulation waves.

A. Verification and Testing of TC Relay Neuron Implementation

According to Equation (A.1), the corresponding parameters of TC relay neuron model are shown in Table I, and the corresponding parameters can be set in the user interface as Figure 5 depicts. The inhibitory synaptic current $I_{Gi\to TC}$ is crucial to the dynamic properties of TC relay neuron. When the value of $I_{Gi\to TC}$ is large, TC relay neurons will have many firing failures and rebound cluster firing behaviors, which destroys their ability to secondary excitatory information in the sensorimotor cortex. Therefore, the models with different $I_{Gi\to TC}$ values can simulate different degrees of pathological behavior of real TC relay neuron.

The TC relay neuron models are implemented on the closed-loop electrophysiology platform, as Figure 6 depicts. DSP1 realizes a parkinsonian TC relay neuron model, which also contains the excitatory input current generation part. DSP2 acts as the digital closed-loop controller, which receives neuron activities (V, ω, etc.) and sends the stimulation signals V_e. The host PC sets the parameters and monitors the crucial signals of models and the controller. TC relay neuron model in parkinsonian state is designed as the controlled neuron due to its abundant dynamics, and the normal TC relay neuron in DSP2 generates the desired signals. The implementation results are shown in Figure 7, where the waveforms generated by the hardware platform are consistent with the MATLAB simulation. Figure 7 (a) is a MATLAB simulation diagram of TC relay neuron's membrane potential (V) both in parkinsonian state ($I_{Gi\to TC} = 4$, upper) and normal state ($I_{Gi\to TC} = 0$, below), and Figure 7 (b) is the corresponding analog oscilloscope picture generated by the hardware platform. The error between the neuron firing waveforms of the hardware platform and the MATLAB software simulation waveforms is 0.0101, which is calculated by Normalized Mean Square Error (NMSE) method:

$$\mathrm{NMSE} = \frac{\sum_{n=1}^{N} \left(f(n) - \hat{f}(n)\right)^2}{\sum_{n=1}^{N} \left(f(n)\right)^2} \tag{3}$$

The stimulation signals V_e in Equation (A.1) are applied to TC relay neurons in the form of electric fields, and the injected current stimulation equivalently perturbs the

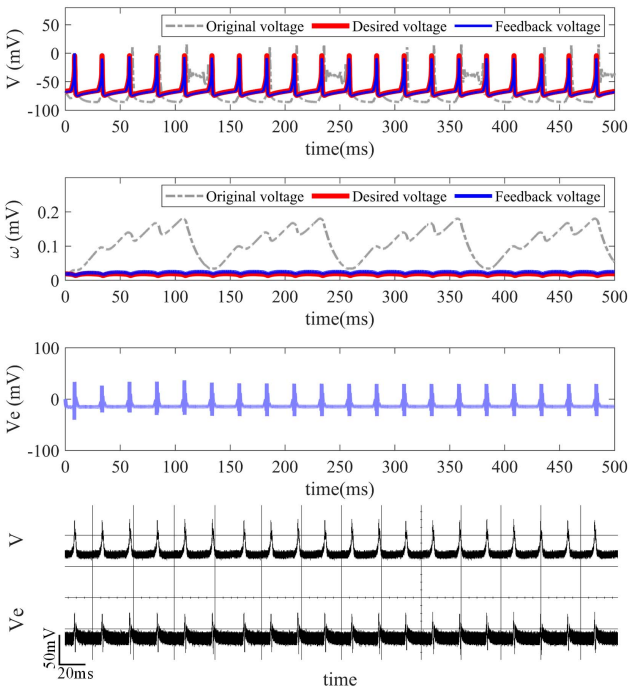

Fig. 9. **Desired stimulation signals acquisition based on membrane potential *V* clamp.** (a) Membrane potential (V) waveform. (b) Gating variable (ω) waveform. (c) Stimulation signal (V_e) waveform. (d) Corresponding hardware waveforms of membrane potential (V) and stimulation signal (V_e).

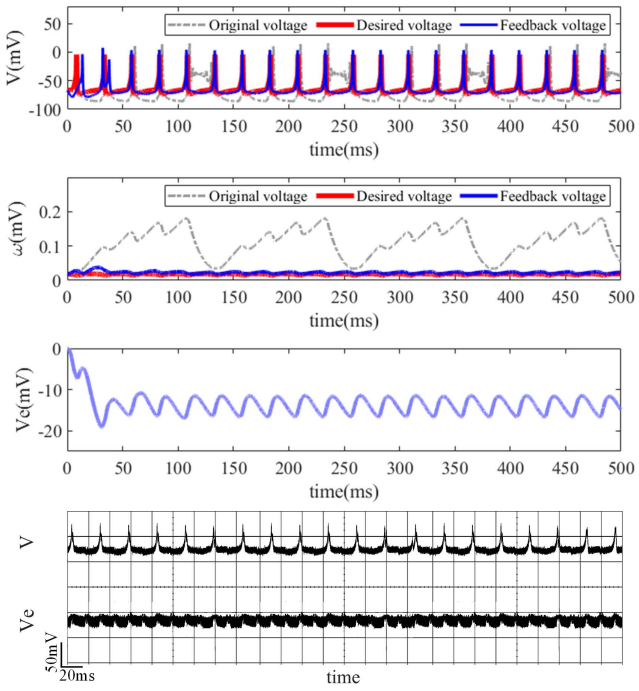

Fig. 10. **Desired stimulation signals acquisition based on ω clamp.** (a) Membrane potential (V) waveform. (b) Gating variable (ω) waveform. (c) Stimulation signal (V_e) waveform. (d) Corresponding hardware waveforms of membrane potential (V) and stimulation signal (V_e).

membrane voltage of TC relay neurons, affecting the magnitude of the respective ion channel currents. To explore the effect of stimulation signals on the model, different open-loop stimulations are applied to TC relay neuron model in parkinsonian state, as Figure 8 shows. By changing the type and the parameters of the stimulation signal V_e, different outputs of membrane potential can be obtained, which verifies the control effect of V_e.

However, the desired outputs based on different requirements are hard to obtain by open-loop stimulation. And different algorithms are required depending on different clamp characteristics and requirements in the electrophysiology experiments. So, the control effect and the applicability of the open-loop stimulation are unstable due to the personalized controlled models in clinical application. Therefore, a closed-loop system is necessary for electrophysiology research.

B. Hardware Closed-Loop Electrophysiological Experiments

1) Desired Stimulation Signals Acquisition Based on Membrane Potential Clamp: PI control law is applied to control the TC relay neuron based on the membrane potential. The stimulation signal V_e is applied to the parkinsonian neuron as a form of external stimulation. In Equation (A.1), $V_e = k_p e + k_i \int e$, where k_p and k_i are the proportional and integral gains, e is the error between the membrane potential V of the desired neuron model and that of the controlled neuron model. In Figure 5, the parameters of PI controller ($k_p = 5, k_i = 0.1$) and the pathological parameter ($I_{Gi\to TC} = 4$) are set in the user interface on the host PC.

As depicted in Figure 9, the membrane potential V and gating variable ω of the controlled parkinsonian TC relay neuron model is consistent with those of desired normal TC relay neuron model after receiving the stimulation signal V_e.

2) Desired Stimulation Signals Acquisition Based on Gating Variable Clamp: In order to research the conductance, synaptic currents as well as architecture of neurons, different clamps are needed to monitor and stimulate neurons. The closed-loop electrophysiology system can also meet the need by changing the clamp to different variables and adjusting the control strategy on the host PC. In this experiment, the clamp is changed to gating variable ω. In Equation (A.1), $V_e = k_p e + k_i \int e$, where k_p and k_i are the proportional and integral gains, e is the error between the gating variable ω of the desired neuron model and that of the controlled neuron model.

As shown in Figure 10, the membrane potential V and gating variable ω of the parkinsonian TC relay model can also be adjusted to the normal state by the stimulation signal V_e. Furthermore, the amplitude of the ω based stimulation signal is smaller than the stimulation signal using membrane potential clamp. More clamps can be selected on the platform, which affect the controller to generate different stimulation signals allowing us to choose the proper stimulation due to the needs.

However, the parameters of PI controller are adjusted based on the trial-and-error method, and the search for suitable parameters requires adequate experience of the user.

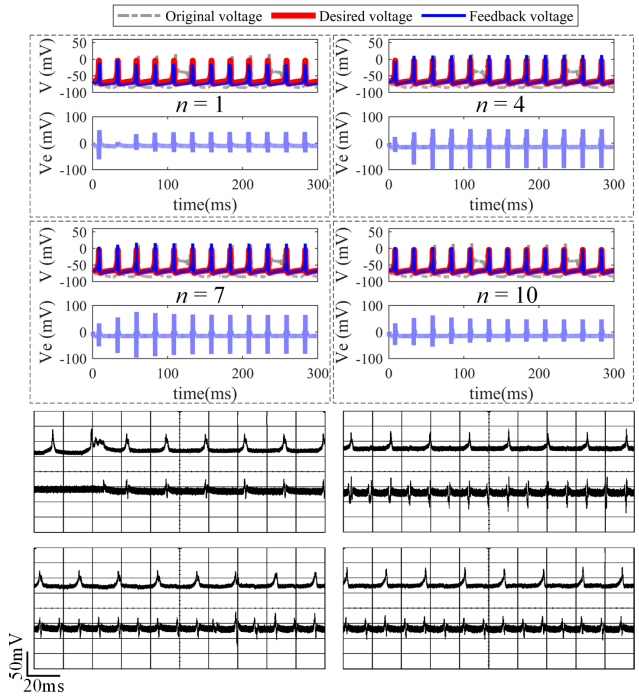

Fig. 11. **The comparison of stimulation performance in different iterative cycle.** (a) Membrane potential (V) waveform and stimulation signal (V_e) waveform in different iteration cycles (n). (b) Corresponding hardware waveforms of membrane potential (V) and stimulation signal (V_e).

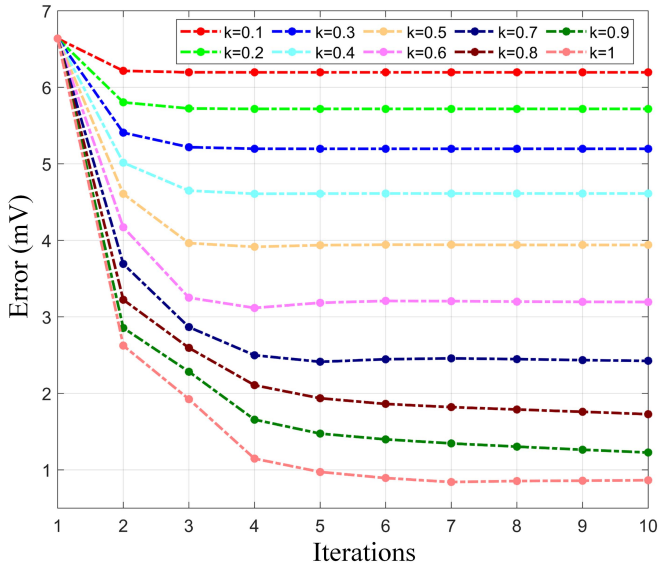

Fig. 12. **The error between the controlled and desired membrane potential under different iteration numbers and iterative control parameter** The error decreases with the increase of the number of iterations, which is faster with larger iterative control parameter k.

C. Performance Test of Closed-Loop Electrophysiology Platform Under Different Complex Situations

1) Desired Stimulation Signals Acquisition Using Proportional-Integral Iterative Learning Control: Due to the high nonlinearity and complexity of nervous system, the established model usually has many uncertain and unknown factors, and the appropriate parameters are difficult to find. When the parameters of PI controller are not suitable, the performance of the simple PI control algorithm is not satisfactory. Since neuronal firing is periodic, the proportional-integral iterative learning control (PI-ILC) algorithm can be used to achieve more effective control of neurons, which is shown in Equation (4):

$$V_e(n+1)(t) = kV_e(n)(t) + k_p e_{n+1}(t) + k_i \int_{t=0}^{T} e_{n+1} dt$$
$$e_{n+1}(t) = y_d(t) - y_{n+1}(t) \quad (4)$$

where T is the time window length of each iteration cycle, $V_e(n)(t)$ is the feedback signal in the nth iteration cycle, $y_{n+1}(t)$ is the output signal, and $y_d(t)$ is the expected signal. k_p and k_i are the proportional and integral gains of the corresponding PI control law [43], [44].

The control strategy can be switched to PI-ILC on the host PC, the clamp is fixed as membrane potential (V), and the parameters of PI-ILC controller are set to an unsuitable value ($k_p = 1.5, k_i = 0$, etc.). The $e_{k+1}(t)$ in Equation (4) is the error of membrane potential V in the (n+1)th iteration between the normal TC relay neuron and the parkinsonian TC relay neuron, and V_e in Equation (A.1) in nth iteration cycle is $V_e(n)(t)$ that calculated by Equation (4).

As Figure 11 depicts, when the number of iterations $n = 1$, only PI control works, the control effect is less than satisfactory. By combining the ILC idea with the classical PI control, the controller superimposes the prior information acquired in the last cycle T and the output stimulation signal V_e of the PI controller to continuously modify the stimulation signal waveforms applied to the TC relay neurons to obtain the continuous attenuation of the system tracking error information. With the PI-ILC control strategy, the membrane potential can track the desired signal gradually without changing the parameter of controller when the number of iterations $n = 10$.

Figure 12 illustrates the trend of the mean error between the controlled membrane potential and desired membrane potential with the number of iterations, and the error decreases with the increase of the number of iterations. Moreover, error decreases faster with larger iterative control parameter k and reaches smaller value after 10 iterations.

2) Different Desired Stimulation Acquisition to Achieve Different Desired Firing Modes: The time patterns issued by neurons can encode different information, which is called as time coding. An important type of time coding is the coding of basic information based on the variation of action potential peaks, called the interspike intervals (ISI) code in neuron discharge string [45], [46].

The ISI of the firing sequence of neurons is often very irregular, but this irregular sequence interval is considered an essential source of neural coding information. At present, the ISI coding method has been widely used to analyze neuronal firing activity. However, the stimulation to achieve different ISI firing mode is hard to obtain. The closed-loop electrophysiology system can also be used to obtain the appropriate

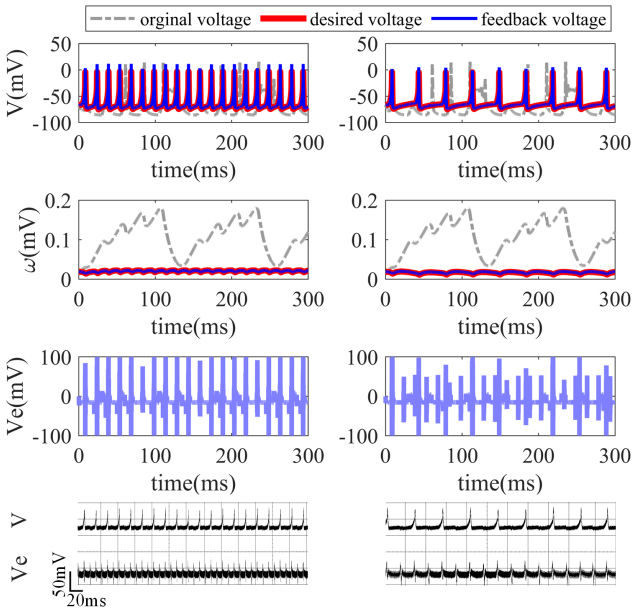

Fig. 13. **The simulation to achieve different desired firing modes.** (a) Membrane potential (V) waveform. (b) Gating variable (ω) waveform. (c) Stimulation signal (V_e) waveform. (d) Corresponding hardware waveforms of membrane potential (V) and stimulation signal (V_e).

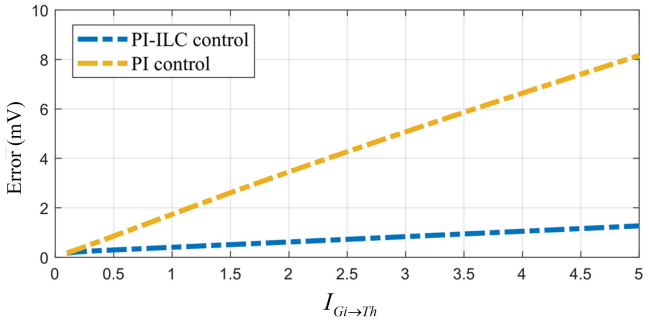

Fig. 14. **The error of PI and PI-ILC control under different pathological parameters.** Pathological parameter is the value of the inhibitory synaptic current $I_{Gi\to TC}$.

stimulation. The ISI of desired model can be changed on the host PC to simulate different firing mode, and the PI-ILC control strategy can be used as the control strategy on the platform.

The $e_{k+1}(t)$ in Equation (4) is the error of the membrane potential V in the $n+1$iteration between the desired TC relay neuron and the parkinsonian TC relay neuron, and the V_e in Equation (A.1) in nth iteration cycle is $V_e(n)(t)$. As is depicted in Figure 13. By using PI-ILC control strategy, both the membrane potential and gating variable of the controlled model can follow the different desired model well without changing the parameters of controller. The stimulation that generates desired firing mode V_e can be obtained by using the closed-loop electrophysiology, which helps us to encode more information in future neuroscience exploration.

3) The Accuracy of Stimulation Effect Using Different Control Strategies: As the disease condition progresses, the update of control parameters may not be timely, resulting in unsatisfactory control effect. The influence of this disturbance on control effect can also be reduced by using PI-ILC. The value of pathological parameter $I_{Gi\to TC}$ can simulate different degrees of pathological behavior of real TC relay neuron, and the value of $I_{Gi\to TC}$ bigger the disease condition worse. By changing $I_{Gi\to TC}$ from 0 to 5 and keeping $k_p = 5$, $k_i = 0.1$ unchanged, we compared the control effect of PI and PI-ILC control strategies with $Error = \frac{1}{m}\sum_{i=0}^{m}|e|$ in Figure 14. Where m is the number of total simulation steps and e is the mean error between the membrane potential V of the desired neuron model and the controlled neuron model. It is evident that the control strategy based on PI-ILC has better robustness and can track desired signals in more complex situations. Furthermore, other different complex control strategies can be extended on the closed-loop electrophysiology system due to different needs in the future.

IV. Conclusion

This paper presents a real-time hardware experiment platform for closed-loop electrophysiology. The platform is implemented on TMS320F28377D DSP, and a corresponding programmable user interface has been designed based on Visual Studio. By using the user interface on host PC, the platform is elastic for users to change models, clamps, desired firing modes, and control strategies to design different experiments. The TC relay neuron model and PI-ILC control are implemented to test and verify the platform in this paper, and the method of TC relay neuron modeling has been discussed in detail to adapt to the platform. We design experiments with different control strategies, different clamps, and different desired firing modes, and the platform can meet the needs of different experiments well. By using the system, researchers can design different experiments on digital neurons to substitute the biological experiment, and the critical data of the target neuron can be stored for the corresponding analysis. The platform is highly compatible, and more neuron models and control strategies can be implemented on the platform to find the appropriate stimulation. Moreover, the correlative work has revealed that the single neuron control scheme can also contribute to the control of neural populations [47], [48], so the system proposed in this study may promote the development of nervous system disease modulation and closed-loop neuroscience.

Appendix A
The Detailed Descriptions and Explanations About Ion Channels, Gated Variables, and Excitatory Input

Ion channel current equations can be described as follows:

$$\begin{aligned} I_{Na} &= g_{Na} m_\infty^3 h\,(V - V_e - E_{Na}) \\ I_K &= g_K 0.75(1-h)^4\,(V - V_e - E_K) \\ I_T &= g_T p_\infty^2\,(V)\,\omega\,(V - V_e - E_T) \\ I_L &= g_L\,(V - V_e - E_L) \end{aligned} \tag{A.1}$$

where V_e is the control voltage that applies to the ion channels. g_i and $E_i (i \in \{Na, K, L, T\})$ represent the maximum

ion channel conductance and the equilibrium back potential, respectively. $P_\infty(V)$ describes the maximum osmotic pressure of the low threshold T-type Ca^{2+} channel membrane.

The gated variables h and ω satisfy the first-order dynamic characteristics:

$$\begin{aligned}\frac{dh}{dt} &= \frac{h_\infty(V)-h}{\tau_h(V)}\\ \frac{d\omega}{dt} &= \frac{\omega_\infty(V)-\omega}{\tau_\omega(V)}\end{aligned} \tag{A.2}$$

where $X_\infty \in \{h_\infty, \omega_\infty\}$ stands for the voltage sensitive steady state variable, $\tau_x \in \{\tau_h, \tau_\omega\}$ is the time constant of each ion channel gating variable.

Furthermore, the steady-state values and time constants of each ion channel variable in the thalamic neuron model can be described by the equation:

$$\begin{aligned} h_\infty(V) &= \frac{1}{1+\exp\left(\frac{V+41}{4}\right)} \quad b_h(V) = \frac{4}{1+\exp\left(-\frac{V+23}{5}\right)}\\ \omega_\infty(V) &= \frac{1}{1+\exp\left(\frac{V+84}{4}\right)} \quad a_h(V) = 0.128\exp\left(-\frac{V+46}{18}\right)\\ m_\infty(V) &= \frac{1}{1+\exp\left(-\frac{V+37}{7}\right)} \quad \tau_h(V) = \frac{1}{a_h(V)+b_h(V)}\\ p_\infty(V) &= \frac{1}{1+\exp\left(-\frac{V+60}{6.2}\right)} \quad \tau_\omega(V) = 28+\exp\left(-\frac{V+25}{10.5}\right)\end{aligned} \tag{A.3}$$

$I_{Gi\to TC}$ is negative with a considerably small value in normal state, while it is much bigger under the abnormal state. A set of periodic rectangular waves are used to describe I_{SM} here, whose expression is as follows:

$$I_{SM} = A_{SM} H\left(\sin\left(\frac{2\pi t}{\rho_{SM}}\right)\right)\left(1-H\left(\sin\left(\frac{2\pi t + D_{SM}}{\rho_{SM}}\right)\right)\right) \tag{A.4}$$

where, parameters A_{SM}, ρ_{SM} and D_{SM} are respectively the amplitude, period, and pulse width of the rectangular wave. $H(x)$ takes Heaviside step function form, when $x < 0$, $H(x) = 0$; When $x > 0$, $H(x) = 1$; When $x = 0$, $H(x) = 0.5$.

Appendix B
The Discrete Analysis of TW Gating Variables h and ω

The discrete analysis of the two gating variables h and ω are as equations show.

$$\begin{cases} h(n+1)-h(n) = \dfrac{h_1(n)}{6}+\dfrac{h_2(n)}{3}+\dfrac{h_3(n)}{3}+\dfrac{h_1(n)}{6}\\ h_1(n) = \Delta t * f(V(n), h(n))\\ h_2(n) = \Delta t * f\left(V(n)+\dfrac{1}{2}V_1(n), h(n)+\dfrac{1}{2}h_1(n)\right)\\ h_3(n) = \Delta t * f\left(V(n)+\dfrac{1}{2}V_2(n), h(n)+\dfrac{1}{2}h_2(n)\right)\\ h_4(n) = \Delta t * f(V(n)+V_3(n), h(n)+h_3(n)) \end{cases} \tag{B.1}$$

$$\begin{cases} \omega(n+1)-\omega(n) = \dfrac{\omega_1(n)}{6}+\dfrac{\omega_2(n)}{3}+\dfrac{\omega_3(n)}{3}+\dfrac{\omega_1(n)}{6}\\ \omega_1(n) = \Delta t * f(V(n), \omega(n))\\ \omega_2(n) = \Delta t * f\left(V(n)+\dfrac{1}{2}V_1(n), \omega(n)+\dfrac{1}{2}\omega_1(n)\right)\\ \omega_3(n) = \Delta t * f\left(V(n)+\dfrac{1}{2}V_2(n), \omega(n)+\dfrac{1}{2}\omega_2(n)\right)\\ \omega_4(n) = \Delta t * f(V(n)+V_3(n), \omega(n)+\omega_3(n)) \end{cases} \tag{B.2}$$

References

[1] J. Decety, "Brain activity during observation of actions. Influence of action content and subject's strategy," *Brain*, vol. 120, no. 10, pp. 1763–1777, Oct. 1997.

[2] D. Papineau, "Neurons and knowledge," *Nature*, vol. 446, no. 7136, pp. 614–615, Apr. 2007.

[3] P. T. Sadtler *et al.*, "Neural constraints on learning," *Nature*, vol. 512, no. 7515, pp. 423–426, 2014.

[4] A. Priori, G. Foffani, L. Rossi, and S. Marceglia, "Adaptive deep brain stimulation (aDBS) controlled by local field potential oscillations," *Exp. Neurol.*, vol. 245, pp. 77–86, Jul. 2013.

[5] P. Svenningsson, E. Westman, C. Ballard, and D. Aarsland, "Cognitive impairment in patients with Parkinson's disease: Diagnosis, biomarkers, and treatment," *Lancet Neurol.*, vol. 11, no. 8, pp. 697–707, Aug. 2012.

[6] J. C. Baldermann *et al.*, "Connectivity profile predictive of effective deep brain stimulation in obsessive-compulsive disorder," *Biol. Psychiatry*, vol. 85, no. 9, pp. 735–743, May 2019.

[7] A. L. Benabid, "Deep brain stimulation for Parkinson's disease," *Current Opinion Neurobiol.*, vol. 13, no. 6, pp. 696–706, 2003.

[8] G. Tinkhauser *et al.*, "The modulatory effect of adaptive deep brain stimulation on beta bursts in Parkinson's disease," *Brain*, vol. 140, pp. 1053–1067, Apr. 2017.

[9] S. W. Moore, P. J. Fox, S. J. Marsh, A. T. Markettos, and A. Mujumdar, "Bluehive—A field-programable custom computing machine for extreme-scale real-time neural network simulation," in *Proc. 20th Int. Symp. Field-Program. Custom Comput. Mach.*, Toronto, ON, Canada, Apr. 2012, pp. 133–140.

[10] Y. Zhang *et al.*, "Brain-inspired computing with memristors: Challenges in devices, circuits, and systems," *Appl. Phys. Rev.*, vol. 7, no. 1, Mar. 2020, Art. no. 011308.

[11] D. Kuzum, R. G. D. Jeyasingh, B. Lee, and H.-S. P. Wong, "Nanoelectronic programmable synapses based on phase change materials for brain-inspired computing," *Nano Lett.*, vol. 12, no. 5, pp. 2179–2186, May 2012.

[12] N. J. Fedorchak, N. Iyer, and R. S. Ashton, "Bioengineering tissue morphogenesis and function in human neural organoids," *Seminars Cell Develop. Biol.*, vol. 111, pp. 52–59, Mar. 2021.

[13] Y. C. Chen *et al.*, "Functional human vascular network generated in photocrosslinkable gelatin methacrylate hydrogels," *Adv. Funct. Mater.*, vol. 22, no. 10, pp. 2027–2039, May 2012.

[14] X. Qian, H. Song, and G.-L. Ming, "Brain organoids: Advances, applications and challenges," *Development*, vol. 146, no. 8, Apr. 2019, Art. no. dev166074.

[15] C. Cea, G. D. Spyropoulos, P. Jastrzebska-Perfect, J. J. Ferrero, J. N. Gelinas, and D. Khodagholy, "Enhancement-mode ion-based transistor as a comprehensive interface and real-time processing unit for *in vivo* electrophysiology," *Nature Mater.*, vol. 19, no. 6, pp. 679–686, Jun. 2020.

[16] J. Modolo, A. Legros, A. W. Thomas, and A. Beuter, "Model-driven therapeutic treatment of neurological disorders: Reshaping brain rhythms with neuromodulation," *Interface Focus*, vol. 1, no. 1, pp. 61–74, Feb. 2011.

[17] O. Faust, U. R. Acharya, H. Adeli, and A. Adeli, "Wavelet-based EEG processing for computer-aided seizure detection and epilepsy diagnosis," *Seizure-Eur. J. Epilepsy*, vol. 26, pp. 56–64, Mar. 2015.

[18] G. Ren, P. Zhou, J. Ma, N. Cai, A. Alsaedi, and B. Ahmad, "Dynamical response of electrical activities in digital neuron circuit driven by autapse," *Int. J. Bifurcation Chaos*, vol. 27, no. 12, Nov. 2017, Art. no. 1750187.

[19] A. Craik, Y. He, and J. L. Contreras-Vidal, "Deep learning for electroencephalogram (EEG) classification tasks: A review," *J. Neural Eng.*, vol. 16, no. 3, Jun. 2019, Art. no. 031001.

[20] B. Rosin *et al.*, "Closed-loop deep brain stimulation is superior in ameliorating Parkinsonism," *Neuron*, vol. 72, pp. 370–384, Oct. 2011.

[21] P. Ghasemi, T. Sahraee, and A. Mohammadi, "Closed- and open-loop deep brain stimulation: Methods, challenges, current and future aspects," *J. Biomed. Phys. Eng.*, vol. 8, no. 2, pp. 209–214, Jul. 2018.

[22] R. Zelmann *et al.*, "CLoSES: A platform for closed-loop intracranial stimulation in humans," *NeuroImage*, vol. 223, Dec. 2020, Art. no. 117314.

[23] X. Wei *et al.*, "An embedded multi-core real-time simulation platform of basal ganglia for deep brain stimulation," *IEEE Trans. Neural Syst. Rehabil. Eng.*, vol. 29, pp. 1328–1340, 2021.

[24] A. O. Hebb *et al.*, "Creating the feedback loop: Closed-loop neurostimulation," *Neurosurg. Clinics*, vol. 25, no. 1, pp. 187–204, Aug. 2014.

[25] L. Grosenick, J. H. Marshel, and K. Deisseroth, "Closed-loop and activity-guided optogenetic control," *Neuron*, vol. 86, no. 1, pp. 106–139, 2015.

[26] Y. Ezzyat *et al.*, "Closed-loop stimulation of temporal cortex rescues functional networks and improves memory," *Nature Commun.*, vol. 9, no. 1, pp. 365–371, Dec. 2018.

[27] C. Liu, J. Wang, H. Li, Z. Xue, B. Deng, and X. Wei, "Model-based iterative learning control of Parkinsonian state in thalamic relay neuron," *Commun. Nonlinear Sci. Numer. Simul.*, vol. 19, pp. 3255–3266, Sep. 2014.

[28] C. Liu, J. Wang, B. Deng, X.-L. Wei, H.-T. Yu, and H.-Y. Li, "Variable universe fuzzy closed-loop control of tremor predominant Parkinsonian state based on parameter estimation," *Neurocomputing*, vol. 151, pp. 1507–1518, Mar. 2015.

[29] B. Shan, J. Wang, B. Deng, X. Wei, H. Yu, and H. Li, "UKF-based closed loop iterative learning control of epileptiform wave in a neural mass model," *Cognit. Neurodyn.*, vol. 9, no. 1, pp. 31–48, Feb. 2015.

[30] S. Yang *et al.*, "Design of hidden-property-based variable universe fuzzy control for movement disorders and its efficient reconfigurable implementation," *IEEE Trans. Fuzzy Syst.*, vol. 27, no. 2, pp. 304–318, Feb. 2019.

[31] X. Hu, C. Liu, L. Liu, J. Ni, and S. Li, "An electronic implementation for Morris-Lecar neuron model," *Nonlinear Dyn.*, vol. 84, no. 4, pp. 2317–2332, 2016.

[32] S. Acciarito *et al.*, "Hardware design of LIF with latency neuron model with memristive STDP synapses," *Integration*, vol. 59, pp. 81–89, Sep. 2017.

[33] Z. Karaca, N. Korkmaz, and Y. Altuncu, "An extensive FPGA-based realization study about the Izhikevich neurons and their bio-inspired applications," *Nonlinear Dyn.*, vol. 105, no. 4, pp. 3529–3549, Sep. 2021.

[34] Y. Yu, F. Han, Q. Wang, and Q. Wang, "Model-based optogenetic stimulation to regulate beta oscillations in parkinsonian neural networks," *Cognit. Neurodyn.*, vol. 4, pp. 1–15, Oct. 2021.

[35] C. Harding, D. A. Bechtold, and T. M. Brown, "Suprachiasmatic nucleus-dependent and independent outputs driving rhythmic activity in hypothalamic and thalamic neurons," *BMC Biol.*, vol. 18, no. 1, pp. 1–16, Sep. 2020.

[36] H.-D. Chehade *et al.*, "Somatosensory thalamic activity modulation by posterior insular stimulation: Cues to clinical application based on comparison of frequencies in a cat model," *Neuromod., Technol. Neural Interface*, vol. 24, no. 2, pp. 229–239, Feb. 2021.

[37] M. R. Romano, R. C. Moioli, and L. A. Elias, "Evaluation of frequency-dependent effects of deep brain stimulation in a cortex-basal ganglia-thalamus network model of Parkinson's disease," in *Proc. 42nd Annu. Int. Conf. Eng. Med. Biol. Soc. (EMBC)*, Jul. 2020, pp. 3638–3641.

[38] V. B. Ho, C. R. Fitz, S. H. Chuang, and C. A. Geyer, "Bilateral basal ganglia lesions: Pediatric differential considerations," *RadioGraphics*, vol. 13, no. 2, pp. 269–292, Mar. 1993.

[39] J. E. Rubin and D. Terman, "High frequency stimulation of the subthalamic nucleus eliminates pathological thalamic rhythmicity in a computational model," *J. Comput. Neurosci.*, vol. 16, no. 3, pp. 211–235, May 2004.

[40] R. Q. So, A. R. Kent, and W. M. Grill, "Relative contributions of local cell and passing fiber activation and silencing to changes in thalamic fidelity during deep brain stimulation and lesioning: A computational modeling study," *J. Comput. Neurosci.*, vol. 32, no. 3, pp. 499–519, Jun. 2012.

[41] K. Kumaravelu, D. T. Brocker, and W. M. Grill, "A biophysical model of the cortex-basal ganglia-thalamus network in the 6-OHDA lesioned rat model of Parkinson's disease," *J. Comput. Neurosci.*, vol. 40, no. 2, pp. 207–229, Apr. 2016.

[42] M. Chen, L. Zu, H. Wang, and F. Su, "FPGA-based real-time simulation platform for large-scale STN-GPe network," *IEEE Trans. Neural Syst. Rehabil. Eng.*, vol. 28, no. 11, pp. 2537–2547, Nov. 2020.

[43] S. Arimoto, S. Kawamura, and F. Miyazaki, "Bettering operation of robots by learning," *J. Robot. Syst.*, vol. 1, no. 2, pp. 123–140, 1984.

[44] P. R. Ouyang, B. A. Petz, and F. F. Xi, "Iterative learning control with switching gain PD feedback for nonlinear systems," in *Proc. IEEE Toronto Int. Conf. Sci. Technol. Hum. (TIC-STH)*, Sep. 2009, pp. 875–880.

[45] V. K. Jirsa, W. C. Stacey, P. P. Quilichini, A. I. Ivanov, and C. Bernard, "On the nature of seizure dynamics," *Brain*, vol. 137, no. 8, pp. 2210–2230, Aug. 2014.

[46] P. Gong, J. Xu, K. Long, and S. Hu, "Chaotic interspike intervals with multipeaked histogram in neurons," *Int. J. Bifurcation Chaos*, vol. 12, no. 2, pp. 319–328, Feb. 2002.

[47] W. Freeman, "Models of the dynamics of neural populations," *Electroencephalogr. Clin. Neurophysiol. Suppl.*, no. 34, pp. 9–18, Jan. 1978.

[48] M. Jazayeri and J. A. Movshon, "Optimal representation of sensory information by neural populations," *Nature Neurosci.*, vol. 9, no. 5, pp. 690–696, May 2006.